Available online at www.sciencedirect.com

ScienceDirect

Energy Procedia 63 (2014) 4289 – 4296

Energy Procedia

GHGT-12

A laboratory study of the elastic and anelastic properties of the sandstone flooded with supercritical CO_2 at seismic frequencies

Vassily Mikhaltsevitch [a,b,*], Maxim Lebedev[a,b], Boris Gurevich[a,b,c]

[a]*Department of Exploration Geophysics, Curtin University, GPO Box U1987, Perth 6845,WA, Australia*
[b]*Cooperative Research Centre for Greenhouse Gas Technologies (CO2CRC), 14-16 Brisbane Avenue, Barton, ACT 2600, Australia*
[c]*CSIRO Earth Science and Resource Engineering, 26 Dick Perry Avenue Kensington, Perth 6151, WA, Australia*

Abstract

The paper studies the influence of supercritical CO_2 ($scCO_2$) on the elastic and inelastic properties of sandstone at seismic frequencies (0.1 - 100 Hz). The seismic frequency experiments were performed with a low-frequency laboratory apparatus utilizing stress-strain relationship, which was developed to measure the complex Young's moduli of rocks at strain amplitudes from 10^{-8} to 10^{-6}. The experiments were conducted on water saturated sandstone (Donnybrook, Western Australia) flooded with $scCO_2$. During the experiments with $scCO_2$ the low-frequency system and the pump with $scCO_2$ were held at a temperature of 42º C. The elastic parameters measured for the sandstone with $scCO_2$ at seismic frequencies are close to those obtained for the dry rock. The extensional attenuation was also measured at seismic frequencies for the dry, water saturated and $scCO_2$-injected sandstone. The applicability of Gassmann's theory to saturated $scCO_2$-water mixture was also explored during the experiments.

Peer-review under responsibility of the Organizing Committee of GHGT-12

Keywords: CO_2; Sequestration; Rock Physics; Attenuation; Elastics

1. Introduction

It is generally accepted that atmospheric carbon dioxide emission is a major negative factor causing global warming and climate change. Geological sequestration, the process of injecting captured CO_2 into deep underground

* Corresponding author. Tel.: +61-8-9266-4976; fax: +61-8-9266-3407.
E-mail address: v.mikhaltsevitch@curtin.edu.au

Peer-review under responsibility of the Organizing Committee of GHGT-12
doi:10.1016/j.egypro.2014.11.464

formations, is regarded as one of the most promising technologies developed to reduce CO_2 concentration in atmosphere. CO_2 injected at a depth of more than 800 meters with suitable porosity and seals, where the gas can be stored in liquid form to reduce the risk of leakage, affects different aspects of storage rocks. Numerous studies demonstrate that CO_2-rock chemical interactions lead to dissolution and precipitation of minerals [1-3] which lead to changes of the petrophysical, mechanical and fluid transport properties of the rocks [4-6].

The seismic effects associated with CO_2 saturation of storage rocks have been a subject of numerous publications in recent years. The effect of CO_2 injection on compressional-wave velocities in hydrocarbon-saturated sandstones was studied in [7], it was found that the experimental velocities are close to the velocities computed using Gassmann's fluid substitution model [8]. The ultrasonic P-wave velocities were measured during CO_2 injection into Tako sandstone in [9] where it was demonstrated that the velocity changes caused by gaseous, liquid, and supercritical CO_2 can be successfully modelled by the Gassmann theory. The experiments undertaken in [10-11] on synthetic and field sandstones at ultrasonic frequencies showed that the Gassmann predictions of both P-wave and S-wave velocities under CO_2 flooding are generally supported by experimental results. The ultrasonic measurements conducted in [12-14] were using seismic difference tomography during the injection of CO_2 into water-saturated Tako sandstone. Xui and Lei [12] found that the patchy saturation model can be used to estimate P-wave velocities if the wavelength of the applied seismic wave is less than the characteristic size of the inhomogeneous patches of CO_2 fractions. Shi et al. [13] reported that the Gassmann equation can be used to predict the P-wave velocity changes caused by $scCO_2$ injection into sandstones if the fluids are mixed at a scale below the critical diffusion length. Lei and Xue [14] showed that their experimental results are in good agreement with the White and Dutta–Odé theory for partial saturation; they also showed that P-wave attenuation increases with CO_2 saturation, achieves a peak at 30-40 % saturation, and then gradually decreases until full CO_2 saturation. The effects of sub-core scale heterogeneity on fluid distribution pattern and acoustic properties of sandstones during imbibition/drainage tests with CO_2/$scCO_2$ were studied by Alemu et al. [15], who indicate that acoustic properties at ultrasonic frequencies can be influenced greater by a fluid distribution pattern than by a variation in CO_2 saturation, and, therefore, the Gassmann theory is not suitable to predict the P- velocity variations. Nakagawa et al. [16] used the split Hopkinson resonant bar method for sonic-frequency (1-2 kHz) measurements of brine-saturated sandstone during $scCO_2$ flooding and demonstrated that changes in acoustic velocities are generally agreed with the Gassmann model. Lebedev et al. [17] investigated acoustic properties of brine-saturated shaly sandstones (the Otway Basin, South Australia) flooded with $scCO_2$ and showed that Gassmann's predictions are in a reasonable agreement with the ultrasonic measurements.

In this paper we present the results of the low-frequency experiments conducted on a water saturated sandstone sample flooded with $scCO_2$. The aim of the experiments was to investigate the effects of $scCO_2$ injection on the elastic and anelastic properties of sandstone at seismic frequencies (0.1 – 100 Hz). The applicability of Gassmann's fluid substitution theory for the interpretation of obtained data was also a subject of our study.

2. Experimental set-up

In this study the experiments at seismic frequencies were performed using a low-frequency laboratory apparatus based on the strain-stress technique with the longitudinal type of the forced oscillations [18-22], which operates at frequencies between 0.01 Hz and 100 Hz and at strain amplitudes from 10^{-8} to 10^{-6} [23]. The apparatus measures the complex Young's moduli of rock samples at confining or uniaxial pressures from 0 to 70 MPa and at pore pressures from 0 to 20 MPa.

The mechanical part of the low-frequency apparatus (Fig. 1a) consists of the frame, formed by two massive steel plates and four poles, and a set of units placed in the center of the frame. The set includes a hydraulic actuator, a Hoek triaxial cell (model 45-D0554, Controls Group), a piezoelectric stack actuator PSt 1000/35/60 (APC International Ltd), an aluminum calibration standard, and two steel plugs with passages for a fluid injection. A specimen to be tested is placed inside a sleeve made of elastomer, which is mounted within the triaxial cell. Two manual hydraulic pumps (model P392, Enerpac) connected with the Hoek cell and hydraulic actuator (model RCS201, Enerpac) provide static lateral and axial forces to the specimen. The use of hydraulic oil as a confining fluid instead of compressed gas (such as nitrogen or helium) allows a very high pressure to be applied safely in the experiment which is an advantage of the apparatus. The dynamic stress applied to the sample and the strains in the

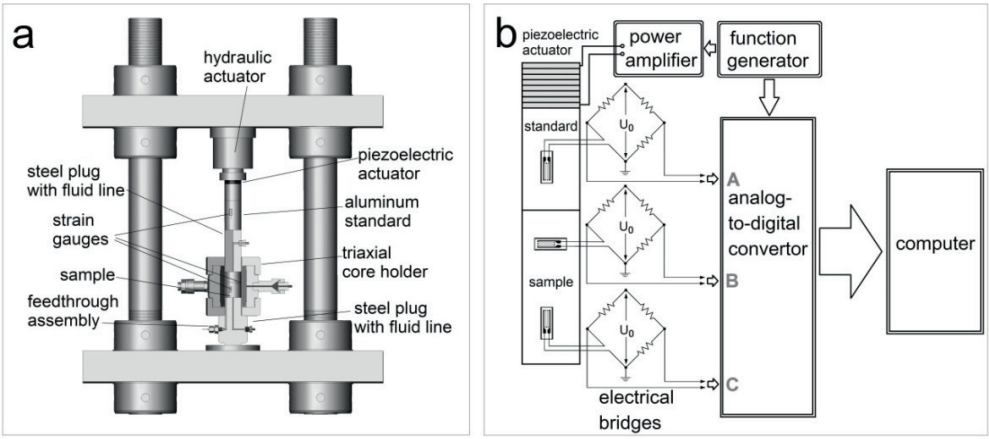

Fig. 1. The mechanical assembly (a) and electrical schematics (b) of the low-frequency laboratory apparatus.

rock are measured by three semiconductor strain gauges (type KSP-6-350-E4, Kyowa Ltd). One gauge is glued to the aluminum standard and the other two glued to the sample with epoxy adhesive (Selleys Araldite Super Strength). The strain gauge on the aluminum standard is orientated in axial direction; the strain gauges attached to the sample are orientated to measure axial and radial strains. The strain gauges are connected with a set of electric bridges (BCM-1 Wheatstone Bridge, Omega Engineering Ltd). The electrical connection of the gauges on the specimen is implemented with a feedthrough assembly (Spectite WFS). To minimize frictions between the strain gages and sleeve, the rock sample is covered by a few layers of teflon tape.

The schematic diagram of the electrical part of the low-frequency apparatus is shown in Fig**.** 1b. The multilayer piezoelectric actuator transforms the periodic voltage, applied by an oscillator, into mechanical stress, which causes displacements in the aluminum standard and tested sample mounted in series.

The displacements modulate the conductivity of the strain gauges. A set of electric bridges transforms the modulated conductivity into electric signals, which, after digitizing by an analogue-to-digital converter (model 100, InstruNet, Omega Engineering Ltd), are received by an acquisition computer, where the signals are averaged and processed. The value of extensional attenuation is derived from the phase delay between the stress applied to the sample and the strain in the rock.

A diagram of the experimental set-up used in this study is presented in Fig. 2. The set-up comprises a CO_2 bottle, a CO_2 syringe pump (model 260D, Teledyne Isco Inc), a low-frequency system, a distilled water container and a pump for water injection (model LC-20AT, Shimadzu Ltd). The water and $scCO_2$ were injected from the bottom end of the sample by the water or CO_2 syringe pump. The pumps were used to control the pore pressure and fluid flow during the experiment.

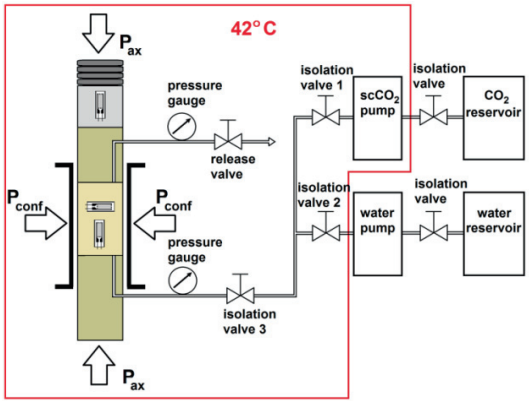

Fig. 2. The arrangement for low-frequency experiments with a water/$scCO_2$ saturated rock sample.

To avoid changes of the elastic parameters of the rock caused by pore pressure variations, the pore pressure was kept constant and the same at both ends of the sample.The Poisson ratio ν and Young's modulus E of each sample were measured by comparing the strains detected in the sandstone and aluminum standard as it is described in [20]. The bulk K and shear μ moduli of the samples can be found by using relations

$$K = \frac{E}{3(1-2\nu)},\ \mu = \frac{E}{2(1+\nu)}\ . \tag{1}$$

In our experiments the extensional attenuation Q_E^{-1} in the sample was measured as a phase shift $\Delta\varphi$ between harmonic stress applied to the sample and resulting strain detected in that sample [24]. We used the following procedure to estimate $\Delta\varphi$. The signals obtained from two axial strain gauges attached to the sample and standard were first averaged and subjected to Fourier transform, then the complex Fourier transform amplitudes of those signals were computed at the frequency of the harmonic stress, and, finally, the target value $\Delta\varphi$ was calculated as the difference between the phases of the found complex amplitudes.

3. Sample description and experimental procedure

In this study we investigated the effects of $scCO_2$ on the acoustic properties of sandstone quarried in Donnybrook, Western Australia. The physical parameters of the sample are as follows: water permeability – 0.28 mD, porosity – 11.54%. The density of the dry sample is 2249 kg/m^3, the density of the water saturated sample is 2364 kg/ m^3.

The physical characteristics of the sandstone and its mineral composition retrieved from X-ray fluorescence and diffraction analysis, are summarised in Table 1. The mineral bulk moduli of the samples were computed using Voigt-Reuss-Hill average [25] on the basis of the bulk moduli of the constituents also given in Table 1 and is equal to 31.7 GPa.

Table 1. The petrographic data for the sandstone sample.

Mineral	Percentage (%)	Bulk Modulus (GPa)
Quartz	60.7	36.6 [25]
Siderite	1.7	117 [26]
Microcline	5.4	55.4 [25]
Plagioclase	9.4	75.6 [25]
Kaolinite	22.8	12 [27]

In case of inhomogeneous rock, the uniformity of the stress in the cross-sections of the rock cannot be ensured and consequently the elastic moduli and extensional attenuation cannot be measured with the stress-strain method. To verify the homogeneity of the sandstone sample, it was scanned using an X-ray microscope VersaXRM-500 (Xradia Ltd). The cross-section scans obtained in three directions are presented in Fig. 3. Based on these X-ray images, we assume that the sandstone tested in this study is homogeneous on a macroscopic (wavelength and sample-size) scale. It is important to note that applicability of our experimental techniques does not require the homogeneity on a microscopic (pore- or grain-size) scale.

The experimental procedure was organized in the following way. First, the sample was vacuum dried at a temperature of 60^0 C for two days. Then a set of low-frequency measurements was conducted in the range of frequencies from 0.1 Hz to 100 Hz at a single differential (confining) pressure of 21 MPa (differential pressure= confining pressure – pore pressure). In the tests with the dry sample the pore pressure did not exceed 0.1 MPa.

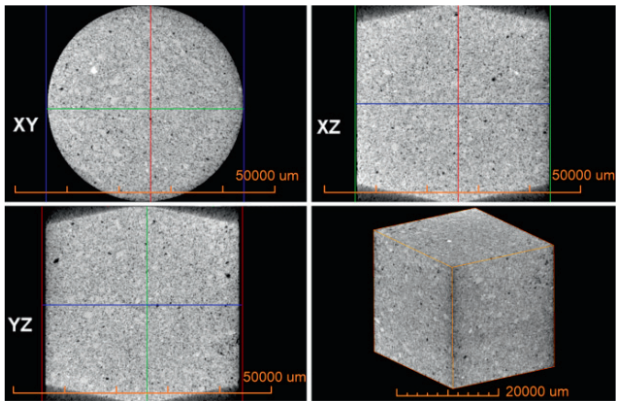

Fig. 3. X-ray scans of the Donnybrook sandstone sample.

After the experiments with the dry rock, the sample was saturated with distilled water by injecting water from the bottom inlet, and the low-frequency tests were conducted again at the same differential pressure of 21 MPa and at a pore pressure of 10 MPa. At the final stage of the low-fgrequency tests, the syringe pump, fluid lines and triaxial cell with the sample inside were heated to a temperature of 42°C and the $scCO_2$ was injected into the sample. The injection lasted for 48 hours at a constant inlet-outlet pressure of 15 MPa to ensure the water in the sandstone is replaced with the maximum amount of the $scCO_2$, during this process the isolation valves 1 and 3 and the release valve (Fig. 2) were open. When the process of saturation was finished, a pore pressure was set up at 10 MPa and all valves were closed. The amount of the residual water in the sample after flooding with $scCO_2$ was estimated at 40% of the pore space by measuring the volume of water removed from the sample.

4. Results

The results of the low-frequency tests are presented in Figures 4-6. Figures 4-5 show the Young's E, Poisson ratio ν, bulk K and shear μ moduli and measured on the dry, water-saturated and $scCO_2$-injected sandstone. The presented results were measured at the differential pressure $P_{diff} = 21$ MPa ($P_{diff} = P_{conf} - P_{pore}$, where P_{conf} and P_{pore} are the confining and pore pressures, correspondingly).

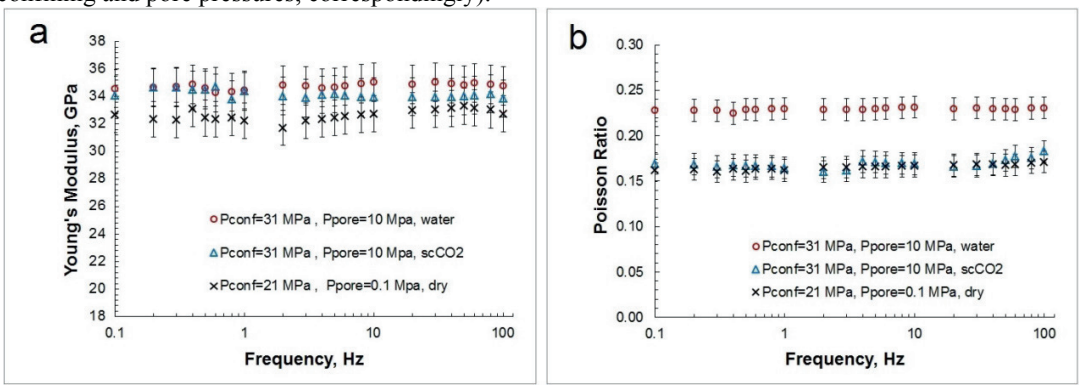

Fig. 4. Young's modulus (a) and Poisson ratio (b) measured for dry, distilled water saturated, and flooded with $scCO_2$ Donnybrook sandstone at the frequency range from 0.1 Hz to 100 Hz.

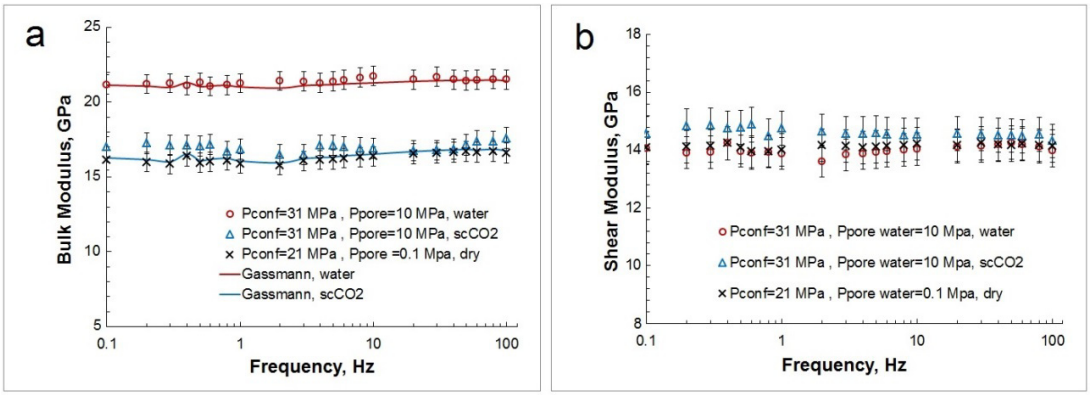

Fig. 5. Bulk (a) and shear (b) moduli measured for dry, distilled water saturated, and flooded with $scCO_2$ Donnybrook sandstone at the frequency range from 0.1 Hz to 100 Hz. The bulk moduli calculated in accordance with the Gassmann equation presented with red (water saturated sandstone) and blue ($scCO_2$ injected sandstone) lines.

In Fig. 5a we compare the low-frequency bulk moduli with the predictions of the Gassmann fluid substitution theory. For our calculations we used the following parameters of $scCO_2$ at a temperature of 42 °C: bulk modulus – 36 MPa, density – 582 kg/m^3.These values were estimated with the Thermophysical Properties of Fluid Systems program developed by the National Institute of Standards and Technology (NIST) [28]. For computing the bulk modulus of the mixture of $scCO_2$ and water, Wood's average [29] was used:

$$K_{\text{mix}} = \left(\frac{S}{K_{\text{water}}} + \frac{1-S}{K_{\text{scCO2}}} \right)^{-1}, \tag{2}$$

where K_{water} and K_{scCO2} are the bulk moduli of water and $scCO_2$, correspondingly, S is the fraction of water in the pores of the rock after $scCO_2$ injection; in our study $S \approx 0.4$.

The bulk moduli of the rock predicted by the Gassmann model were found in accordance with the relation [8]:

$$K_{\text{sat}} = K_{\text{dry}} + \frac{\left(1 - \frac{K_{\text{dry}}}{K_{\text{min}}}\right)^2}{\frac{\phi}{K_{\text{mix}}} + \frac{1-\phi}{K_{\text{min}}} - \frac{K_{\text{dry}}}{K_{\text{min}}^2}}, \tag{3}$$

where K_{dry} and K_{sat} are the dry and fluid saturated bulk moduli, respectively, K_{min} is the bulk modulus of the minerals forming the rock, ϕ is the rock porosity. The fact that the bulk and shear moduli of the sample flooded with $scCO_2$ are not frequency dependent suggests that the pressures in the pores filled with water or $scCO_2$-water mixture are in equilibrium for frequencies between 0.1 Hz and 100 Hz. According to the principle of causality, presented for linear viscoelastic systems by the Kramers-Kronig relations [30], the absence of significant moduli dispersion should correspond to insignificant attenuation which is consistent with our experimental data. The results presented in Fig. 6a demonstrate that the extensional attenuation measured in the water saturated sandstone before and after $scCO_2$ injection is scarcely above the experimental error.

The seismic compressional V_P and shear V_S velocities presented in Fig. 6b were computed using the following equations:

$$V_p = \sqrt{\frac{E(1-\nu)}{(1+\nu)(1-2\nu)\rho}}, \quad V_S = \sqrt{\frac{E}{2(1+\nu)\rho}}. \tag{4}$$

where ρ is the density of the sandstone. The differences in P-wave velocities are caused by the contrast in the densities of the pore fluids.

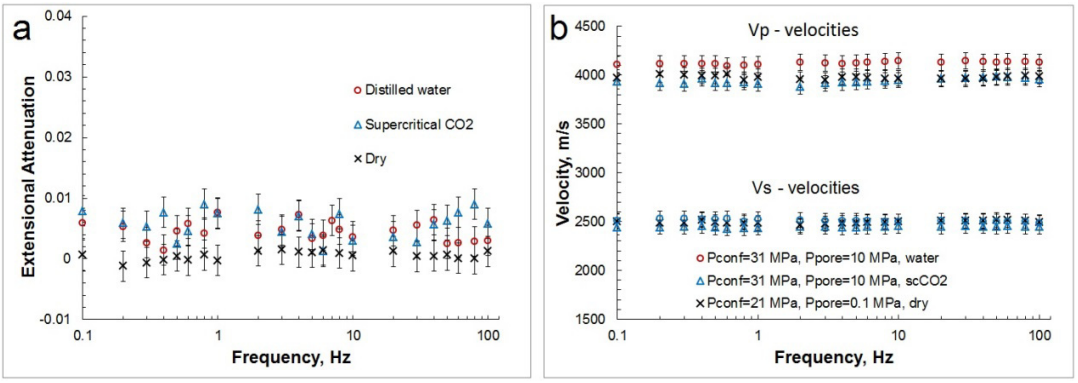

Fig. 6. Extensional attenuation (a) and seismic velocities (b) obtained for dry, distilled water saturated and flooded with $scCO_2$ sandstone.

5. Conclusions

The elastic properties and extentional attenuation of low-permeability sandstone (Donnybrook, Western Australia) were measured at seismic frequencies of 0.1 Hz to 100 Hz during flooding tests with distilled water and $scCO_2$. At first the experiments were carried out with the dry and water saturated sandstone at a temperature of 22 º C. Then the Hoek triaxial cell with the water saturated sample inside, the pump comprising $scCO_2$ and fluid lines were heated to a temperature of 42º C and the sample was flooded with $scCO_2$. The amount of the water in the sample after flooding with $scCO_2$ was estimated at 40% of the pore space.

In our experiments we found a reduction of ~5 % in P-velocities at a differential pressure of 21 MPa after $scCO_2$ injection which agrees with the difference in P-velocity between the water saturated and dry sample. We found that the extensional attenuation measured in the water saturated sandstone before and after $scCO_2$ injection is practically unchanged.

In our tests we also found that the elastic parameters measured for the $scCO_2$ injected rock are very close to the elastic parameters measured of the same rock in dry state.

Our analysis shows that the Gassmann fluid substitution theory is applicable for the interpretation of the data measured on the Donnibrook sandstone in flooding tests with $scCO_2$.

Acknowledgments

This work was partially funded by the Australian Commonwealth Government through the Cooperative Research Centre for Greenhouse Gas Technologies (CO2CRC) and by the sponsors of the Curtin Reservoir Geophysics Consortium (CRGC). The authors thank the National Geosequestration Laboratory (NGL) for providing access to the X-ray microscope VersaXRM-500 (Xradia Ltd). The NGL is a collaboration between CSIRO, the University of Western Australia and Curtin University established to conduct and deploy critical research and development to enable commercial-scale carbon storage options. Funding for this facility was provided by the Australian Federal Government. The authors greatly thank Dr Yulia Uvarova for the petrographic analysis of Donnybrook sandstone.

References

[1] Le Guen Y, Renard F, Hellmann R, Brosse E, Collombet M, Tisserand D, Gratier J-P. Enhanced deformation of limestone and sandstone in the presence of high P_{CO2} fluids. *J Geophys Res Sol Ea* 2007; 112: B05421

[2] Zemke K, Liebscher A, Wandrey M. Petrophysical analysis to investigate the effects of carbon dioxide storage in a subsurface saline aquifer at Ketzin, Germany (CO_2SINK). *Int J Greenh Gas Con* 2010; 4: 990-999.

[3] Nover G, Von Der Gönna J, Heikamp S, Köster J. Changes of petrophysical properties of sandstones due to interaction with supercritical carbon dioxide – a laboratory study. *Eur J Miner* 2013; 25: 317-329.

[4] Rochelle CA, Czernichowski-Lauriol I, Milodowski AE. The impact of chemical reactions on CO_2 storage in geological formations: a brief review. In: Baines SJ, Worden RH, editors. *Geological Storage of Carbon 233,* London: Geological Society, Special Publications; 2004. p. 87-106.

[5] Vialle S, Vanorio T. Laboratory measurements of elastic properties of carbonate rocks during injection of reactive CO_2 - saturated water. *Geophys Res Lett* 2011; 38: L01302
[6] Hangx S, Van der Linden A, Marceils F, Bauer A. The effect of CO_2 on the mechanical properties of the Captain Sandstone: Geological storage of CO_2 at the Goldeneye field (UK). *Int J Greenh Gas Con* 2013; 19: 609-619.
[7] Wang Z, Nur A. Effect of CO_2 flooding on wave velocities in rocks and hydrocarbons. *SPE Reservoir Eng* 1989; 4: 429–439.
[8] Gassmann F. Über die elastizität poröser medien. *Viertel. Naturforsch. Ges. Zürich*, 1951; 96: 1–23.
[9] Xue Z, Ohsumi T. Seismic wave monitoring of CO_2 migration in water-saturated porous sandstone. *Explor Geophys* 2004; 35: 25–32.
[10] Siggins AF. Velocity-effective stress response of CO_2-saturated sandstones. *Explor Geophys* 2006; 37: 60–66.
[11] Siggins AF, Lwin M, Wisman P. Laboratory calibration of the seismo-acoustic response of CO_2 saturated sandstones. *Int J Greenh Gas Con* 2010; 4: 920–927.
[12] Xue Z, Lei X. Laboratory study of CO_2 migration in water-saturated anisotropic sandstone, based on P-wave velocity imaging. *Explor Geophys* 2006; 37: 10–18.
[13] Shi J-Q, Xue Z, Durucan S. Seismic monitoring and modelling of supercritical CO_2 injection into a water-saturated sandstone: Interpretation of P-wave velocity data. *Int J Greenh Gas Con* 2007; 1: 473–480.
[14] Lei X, Xue Z. Ultrasonic velocity and attenuation during CO_2 injection into water-saturated porous sandstone: Measurements using difference seismic tomography. *Phys Earth Planet In* 2009; 176: 224–234.
[15] Alemu BL, Aker E, Soldal M, Johnsen Ø, Aagard P. Effect of sub-core scale heterogeneities on acoustic and electrical properties of a reservoir rock: a CO_2 flooding experiment of brine saturated sandstone in a computed tomography scanner. *Geophys Prospect* 2013; 61: 235-250.
[16] Nakagawa S, Kneafsey TJ, Daley TM, Freifeld BM, Rees EV. Laboratory seismic monitoring of supercritical CO_2 flooding in sandstone cores using the split Hopkinson resonant bar technique with concurrent X-ray computed tomography imaging. *Geophys Prospect* 2013; 61: 254–269.
[17] Lebedev M, Pervukhina M, Mikhaltsevitch V, Dance T, Bilenko O, Gurevich B. An experimental study of acoustic responses on the injection of supercritical CO_2 into sandstones from the Otway Basin. *Geophysics* 2013; 78: D293-D306.
[18] Spencer JW. Stress relaxation at low frequencies in fluid-saturated rocks: Attenuation and modulus dispersion. *J Geophys Res* 1981; 86: 1803–1812.
[19] Paffenholz J, Burkhardt H. Absorption and modulus measurements in the seismic frequency and strain range on partially saturated sedimentary rocks. *J Geophys Res* 1989; 94: 9493–9507.
[20] Batzle ML, Han D-H, Hofmann R. Fluid mobility and frequency-dependent seismic velocity - Direct measurements. *Geophysics* 2006; 71: N1–N9.
[21] Takei Y, Fujisawa K, McCarthy C. Experimental study of attenuation and dispersion over a broad frequency range: 1. The apparatus. *J Geophys Res* 2011; 116: B09204.
[22] Tisato N. and Madonna C. 2012. Attenuation at low seismic frequencies in partially saturated rocks: Measurements and description of a new apparatus. *Journal of Applied Geophysics* **86**, 44–53
[23] Mikhaltsevitch V, Lebedev M, Gurevich B. A laboratory study of low-frequency wave dispersion and attenuation in water-saturated sandstones. *The Leading Edge* 2014; 33: 616 – 622.
[24] O'Connell RJ, Budiansky B. Measures of dissipation in viscoelastic media. *Geophys Res Lett* 1978; 5: 5–8.
[25] Mavko G, Mukerji T, Dvorkin J. The Rock Physics Handbook: Tools for Seismic Analysis of Porous Media. 2nd ed. Cambridge: Cambridge University Press; 2009.
[26] Zhang J, Martinez I, Guyot F, Reeder RJ. Effects of Mg-Fe^{2++} substitution in calcite-structure carbonates: Thermoelastic properties. *Am Mineral* 1998; 83: 280 – 287.
[27] Vanorio T, Prasad M, Nur A. Elastic properties of dry clay mineral aggregates, suspensions and sandstones. *Geophys J Int* 2003; 155: 319 – 326.
[28] Lemmon E, McLinden M, Friend D. Thermophysical properties of fluid systems. In: Linstrom PJ, Mallard WG, editors. NIST Chemistry WebBook: National Institute of Standards and Technology, http://webbook.nist.gov; 2011. NIST Standard Reference Database Number 69.
[29] Wood AW. A Textbook of Sound. New York: McMillan Co; 1955.
[30] O'Donnel M, Jaynes ET, Miller JG. Kramers – Kronig relationship between ultrasonic attenuation and phase velocity. *J Acoust Soc Am* 1981; 69: 696–701.